related to the context or shock but did not encode the contextual fear memory.

If the retrieval induces the destabilization of the preexisting memory, it would also occur in the extinction, which is produced by repetitive retrievals in the absence of unconditioned stimuli. To test this idea, we performed the extinction training for 2 days, with two spaced retrievals per day (*25*). Either vehicle or βlac was infused immediately after the retrievals, and the freezing level was tested on the third day (Fig. 4C). It is noteworthy that βlac infusions into area CA1 suppressed the extinction of contextual fear memory (Fig. 4D and fig. S4B). The freezing behavior was significantly reduced by the extinction in the animals reexposed to the context with vehicle infusions, whereas control animals without context reexposure showed no extinction (Fig. 4D and fig. S4B). Thus, our data suggest that ubiquitin- and proteasome-dependent protein degradation is required for the memory extinction. This supports the idea that extinction is not only "inhibitory new learning" of a context–no shock association, but also involves at least some "unlearning" (or forgetting) of the preexisting context-shock association (*26*, *27*). Furthermore, extinction has been suggested to involve a memory-updating process (*27*). Combined, our results support the idea that memory retrieval makes preexisting memory labile via ubiquitin- and proteasome-dependent protein degradation in order to update or reorganize the memory with new information.

Our data also showed that infusion of βlac alone immediately after conditioning did not impair the acquisition of fear memory. This result disagrees with previous studies in some aspects (*14*, *28*). In these studies, the consolidation of inhibitory avoidance or contextual fear memory is impaired by disturbance of the ubiquitin and proteasome pathway. These discrepancies may reflect the differences in the experimental system, animal species, or brain regions involved (*29*). It is known that the circuits involved in the processing of an inhibitory avoidance task are somewhat different from the circuits of classical fear conditioning (*30*). Moreover, in contextual fear conditioning, three variables—reexposure duration, the age of the memory, and the strength of the memory—influence the memory processes activated during retrieval (*2*).

NMDA receptor activation triggers the destabilization of the consolidated fear memory (*8*). In cultured neurons, glutamatergic transmission activates the ubiquitin and proteasome system (*31*, *32*). It would be interesting to speculate that ubiquitin- and proteasome-dependent protein degradation is increased by downstream signaling of NMDA receptor activation and destabilizes the retrieved fear memory.

We have shown that ubiquitin- and proteasome-dependent degradation of preexisting postsynaptic proteins is involved in memory reorganization after retrieval. Our results support the idea that memory reorganization occurs via both degradation of preexisting synapses and synthesis of updated synapses. Preexisting memory may be rebuilt in conjunction with new information via the protein degradation and concurrent synthesis especially in the synaptic region.

References and Notes

1. K. Nader, G. E. Schafe, J. E. Le Doux, *Nature* **406**, 722 (2000).
2. A. Suzuki *et al.*, *J. Neurosci.* **24**, 4787 (2004).
3. M. H. Milekic, C. M. Alberini, *Neuron* **36**, 521 (2002).
4. P. W. Frankland *et al.*, *Learn. Mem.* **13**, 451 (2006).
5. C. M. Alberini, *Trends Neurosci.* **28**, 51 (2005).
6. R. G. Morris *et al.*, *Neuron* **50**, 479 (2006).
7. Y. Dudai, *Curr. Opin. Neurobiol.* **16**, 174 (2006).
8. C. Ben Mamou, K. Gamache, K. Nader, *Nat. Neurosci.* **9**, 1237 (2006).
9. M. Eisenberg, T. Kobilo, D. E. Berman, Y. Dudai, *Science* **301**, 1102 (2003).
10. O. Steward, E. M. Schuman, *Annu. Rev. Neurosci.* **24**, 299 (2001).
11. M. D. Ehlers, *Nat. Neurosci.* **6**, 231 (2003).
12. A. N. Hegde *et al.*, *Cell* **89**, 115 (1997).
13. A. N. Hegde, A. L. Goldberg, J. H. Schwartz, *Proc. Natl. Acad. Sci. U.S.A.* **90**, 7436 (1993).
14. M. Lopez-Salon *et al.*, *Eur. J. Neurosci.* **14**, 1820 (2001).
15. R. Fonseca, R. M. Vabulas, F. U. Hartl, T. Bonhoeffer, U. V. Nagerl, *Neuron* **52**, 239 (2006).
16. E. R. Kandel, *Science* **294**, 1030 (2001).
17. A. Ciechanover, *Nat. Rev. Mol. Cell Biol.* **6**, 79 (2005).
18. Q. Deveraux, V. Ustrell, C. Pickart, M. Rechsteiner, *J. Biol. Chem.* **269**, 7059 (1994).
19. K. Ferrell, Q. Deveraux, S. van Nocker, M. Rechsteiner, *FEBS Lett.* **381**, 143 (1996).
20. Materials and methods are available as supporting material on *Science* Online.
21. C. Luscher, R. A. Nicoll, R. C. Malenka, D. Muller, *Nat. Neurosci.* **3**, 545 (2000).
22. S. Lim *et al.*, *J. Biol. Chem.* **274**, 29510 (1999).
23. J. A. Lee *et al.*, *J. Cell Biol.* **174**, 827 (2006).
24. T. Abel, K. C. Martin, D. Bartsch, E. R. Kandel, *Science* **279**, 338 (1998).
25. K. M. Lattal, T. Abel, *J. Neurosci.* **21**, 5773 (2001).
26. K. M. Myers, M. Davis, *Neuron* **36**, 567 (2002).
27. J. Ji, S. Maren, *Hippocampus* **17**, 749 (2007).
28. Y. H. Jiang *et al.*, *Neuron* **21**, 799 (1998).
29. S. J. Martin, P. D. Grimwood, R. G. Morris, *Annu. Rev. Neurosci.* **23**, 649 (2000).
30. A. E. Wilensky, G. E. Schafe, J. E. LeDoux, *J. Neurosci.* **20**, 7059 (2000).
31. B. Bingol, E. M. Schuman, *Nature* **441**, 1144 (2006).
32. L. Guo, Y. Wang, *Neuroscience* **145**, 100 (2007).

33. We thank E. Kandel, A. Silva, P. Frankland, S. Josselyn, and Y.-S. Lee for reading the manuscript and critical discussion. We are grateful to lab members for their technical help. We also thank E. Kim for providing Shank antibody. This work was supported by the Creative Research Initiative Program of the Korean Ministry of Science and Technology (to B.-K.K.).

Supporting Online Material

www.sciencemag.org/cgi/content/full/1150541/DC1
Materials and Methods
Figs. S1 to S5
References

14 September 2007; accepted 11 January 2008
Published online 7 February 2008;
10.1126/science.1150541
Include this information when citing this paper.

Hybrid Neurons in a MicroRNA Mutant Are Putative Evolutionary Intermediates in Insect CO_2 Sensory Systems

Pelin Cayirlioglu,[1]* Ilona Grunwald Kadow,[1]*† Xiaoli Zhan,[1] Katsutomo Okamura,[2] Greg S. B. Suh,[3]‡ Dorian Gunning,[1] Eric C. Lai,[2] S. Lawrence Zipursky[1]§

Carbon dioxide (CO_2) elicits different olfactory behaviors across species. In *Drosophila*, neurons that detect CO_2 are located in the antenna, form connections in a ventral glomerulus in the antennal lobe, and mediate avoidance. By contrast, in the mosquito these neurons are in the maxillary palps (MPs), connect to medial sites, and promote attraction. We found in *Drosophila* that loss of a microRNA, *miR-279*, leads to formation of CO_2 neurons in the MPs. *miR-279* acts through down-regulation of the transcription factor Nerfin-1. The ectopic neurons are hybrid cells. They express CO_2 receptors and form connections characteristic of CO_2 neurons, while exhibiting wiring and receptor characteristics of MP olfactory receptor neurons (ORNs). We propose that this hybrid ORN reveals a cellular intermediate in the evolution of species-specific behaviors elicited by CO_2.

In insects, both the position of CO_2 neurons and the behavior elicited by CO_2 differ among species. For example, olfactory detection of CO_2 through neurons positioned in or around the mouthparts of an insect, such as maxillary palps (MPs) and labial palps, correlates with feeding-related behaviors. Indeed, in some blood-feeding insects such as mosquitoes and tsetse flies, these neurons are harbored in the MPs and are important in locating hosts via plumes of CO_2 that they emit (*1*–*3*). The hawkmoth, *Manduca sexta*, monitors nectar profitability of newly opened *Datura wrightii* flowers through CO_2 receptor neurons located in their labial palps (*4*, *5*). In these examples, CO_2 acts as an attractant. Conversely, in *Drosophila* CO_2 is a component of a stress-induced odor that triggers avoidance behavior (*6*). This repellent response is driven by antennal neurons expressing the CO_2 receptor complex Gr21a-Gr63a (*7*, *8*). How did these diverse behavioral responses to CO_2 arise during insect evolution? We propose that this diversity emerged through multiple steps, including changes in cellular position (arising from elimination of CO_2 neurons in one appendage and generation of these neurons in another) and changes in circuitry.

Downloaded from http://science.sciencemag.org/ on October 17, 2017

In the course of a genetic screen for mutants disrupting the organization of the olfactory system, we isolated a mutant (*S0962-07*) that resulted in the formation of ectopic Gr21a-expressing neurons in the MPs (Fig. 1A). Some 22 ± 1.5 (mean ± SEM) green fluorescent protein (GFP)–positive cells were observed in the mutant MP, whereas the number of antennal Gr21a olfactory receptor neurons (ORNs) was unaffected (Fig. 1B). In the wild type, Gr21a cell bodies were restricted to the antenna (Fig. 1A). The ectopic MP cells expressed both CO_2 receptors (Gr21a and Gr63a) (Fig. 1C). Consistent with this finding, mutant cells conferred CO_2 sensitivity to the MP (Fig. 1D). Staining the MP with an antibody to the pan-neuronal marker Elav revealed an increase of 21 ± 3.4 neurons in the mutant, which suggests that all ectopic neurons expressed Gr21a (fig. S1).

In wild-type MPs, each sensillum contains two ORNs. By contrast, in the mutant MP sensilla, additional neurons expressing Elav and the general receptor Or83b were observed (Fig. 1E and fig. S1). This was also apparent when a MP ORN marker (MPS-GAL4) expressed in a subset of MP ORNs was used (Fig. 1E) (*9*). This marker labels single cells within a subset of wild-type MP sensilla (Fig. 1E, arrows); however, in mutant MPs, two additional neurons were observed (Fig. 1E, arrowheads), bringing the total number of neurons within these sensilla to four. Thus, the generation of ectopic Gr21a-Gr63a neurons is due to an increase in the number of neurons within sensilla rather than transformation of MP ORNs (fig. S1).

In the wild type, each class of adult ORNs sends projections from both antennae or MPs to the antennal lobe (AL). ORNs expressing same odorant receptors (ORs) typically form synapses in the same glomerulus within the AL (fig. S2) (*10*). CO_2 neurons in the antenna target the V-glomerulus (Fig. 1F). To specifically assess the targeting of ectopic MP CO_2 neurons, we examined flies where the antennae were surgically removed (Fig. 1F). We found that ectopic CO_2 neurons targeted the V-glomerulus and other medial sites in the AL (Fig. 1F; see also below). The wiring specificity of antennal CO_2 neurons in the mutants was identical to that in the wild type (Fig. 1F). Thus, the ectopic CO_2 neurons in the MP target, at least in part, the same glomerulus innervated by the wild-type CO_2 neurons in the antennae.

We mapped *S0962-07* to a P-element insertion some 1 kb upstream of a microRNA, *miR-279* (fig. S3). MicroRNAs (miRNAs) are small noncoding RNAs of about 22 nucleotides that bind to specific sequences of the 3′-untranslated region (3′UTR) of target genes and thereby repress gene expression posttranscriptionally. In recent years, miRNAs were implied in a variety of functions in the nervous system of different organisms (*11*). To assess whether *miR-279* is responsible for the observed phenotype, we generated three small deletions that uncovered the *miR-279* genomic region (fig. S3). These deletion mutants exhibited phenotypes indistinguishable from *S0962-07* (fig. S3). The ectopic CO_2 phenotype was rescued by a 3-kb fragment of genomic DNA encoding only *miR-279* (fig. S3) (*9*). Thus, *miR-279* is the gene disrupted in *S0962-07* and must repress targets in the MP to inhibit ectopic CO_2 neuron development.

To assess whether *miR-279* is expressed in the developing MPs, we generated transgenic

[1]Department of Biological Chemistry, Howard Hughes Medical Institute, David Geffen School of Medicine, University of California, Los Angeles, CA 90095, USA. [2]Sloan-Kettering Institute, 521 Rockefeller Research Labs, 1275 York Avenue, Box 252, New York, NY 10021, USA. [3]Division of Biology 216-76, California Institute of Technology, Pasadena, CA 91125, USA.

*These authors contributed equally to this work.
†Present address: Department of Molecular Neurobiology, Max Planck Institute of Neurobiology, Am Klopferspitz 18, 82152 Martinsried, Germany.
‡Present address: Molecular Neurobiology Program, Skirball Institute, Department of Cell Biology, New York University School of Medicine, New York, NY 10016, USA.
§To whom correspondence should be addressed. E-mail: lzipursky@mednet.ucla.edu

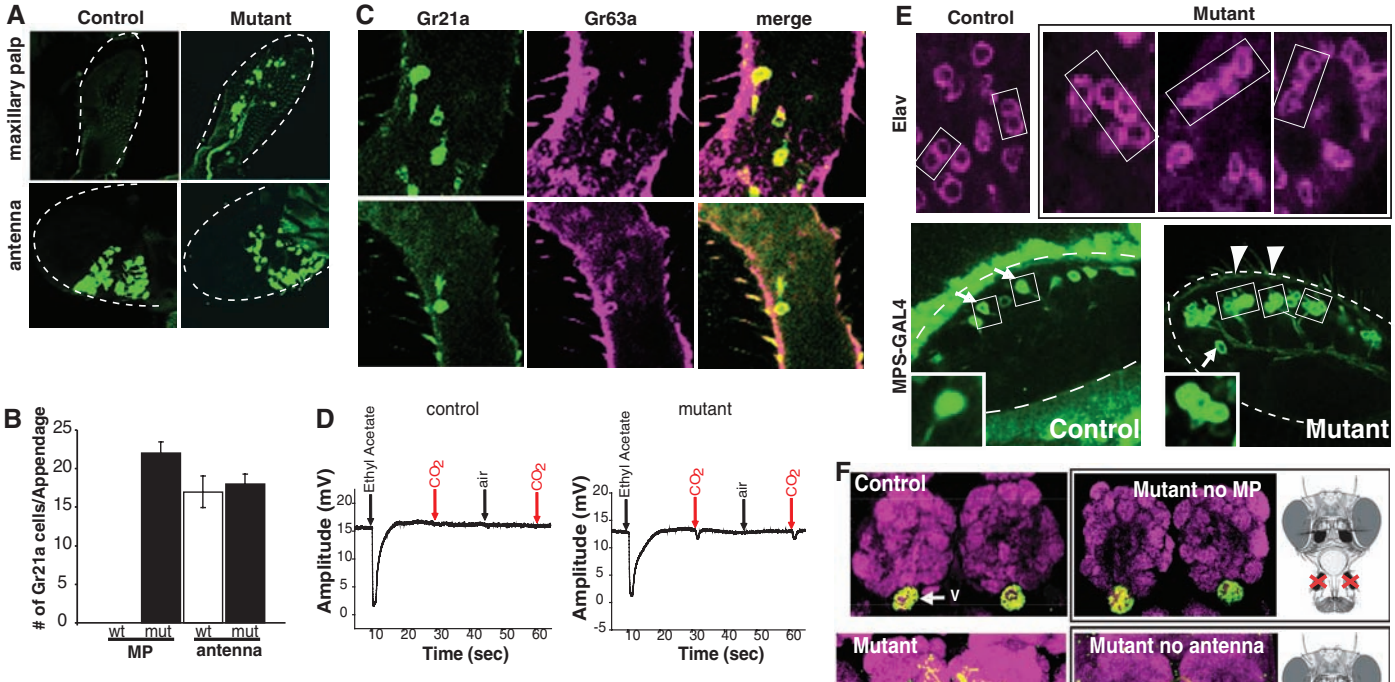

Fig. 1. Ectopic CO_2 neurons are formed in the MPs of *S0962-07* mutants. (**A**) Gr21a expression in wild-type and mutant olfactory appendages. (**B**) Quantification of Gr21a-positive cells in the MP and antenna. (**C**) Gr63a (magenta, RNA antisense probe) and Gr21a (green, Gr21a-GAL4) are coexpressed in the MP. (**D**) Electropalpograms comparing the response to ethyl acetate, air, and CO_2 in control and mutant flies. Contrary to lack of response from the control palps, 5 of 12 mutant MPs responded to CO_2 (*9*). MPs recorded: $n = 12$ (control), $n = 12$ (mutant), $P = 0.016$. (**E**) Single confocal sections of MPs labeled with antibody to Elav (magenta) at 60 to 80 hours APF or with MPS-GAL4 and UAS-mCD8GFP (green) at 80 hours APF. Two neurons (Elav) or single ORNs (MPS-GAL4) are labeled in wild-type MP sensilla (arrows). Two additional neurons are observed in a subset of mutant sensilla (arrowheads and inset). (**F**) Mutant neurons in the MP target the V and medial glomeruli. Mutant flies without MP (upper right) and without antenna (lower right). Magenta, anti-NC82. In (A) and (E), dashed lines outline MPs.

Downloaded from http://science.sciencemag.org/ on October 17, 2017

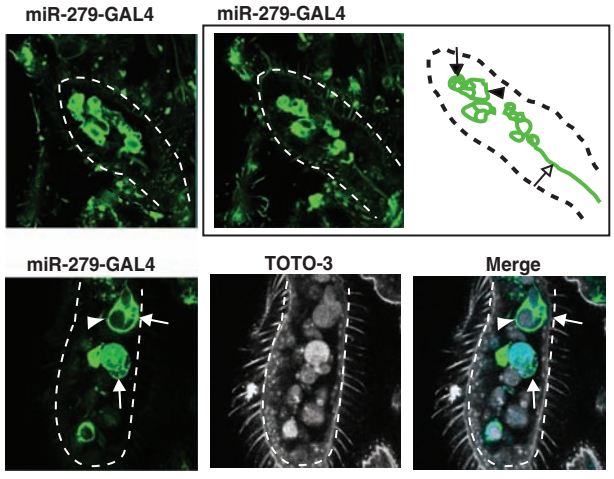

Fig. 2. *miR-279* is expressed in precursor cells in the developing MP. Expression of *miR-279* was visualized with miR-279-GAL4 and UAS-CD8GFP (green). The arrowhead and arrow in both the schematic and the image panels point to a big cell and a cluster of small cells, respectively. The open arrow in the schematic points to a nerve fiber from one of the cell clusters. Nuclear counterstain TOTO-3 is used in the bottom panels. Dashed lines outline the developing MPs.

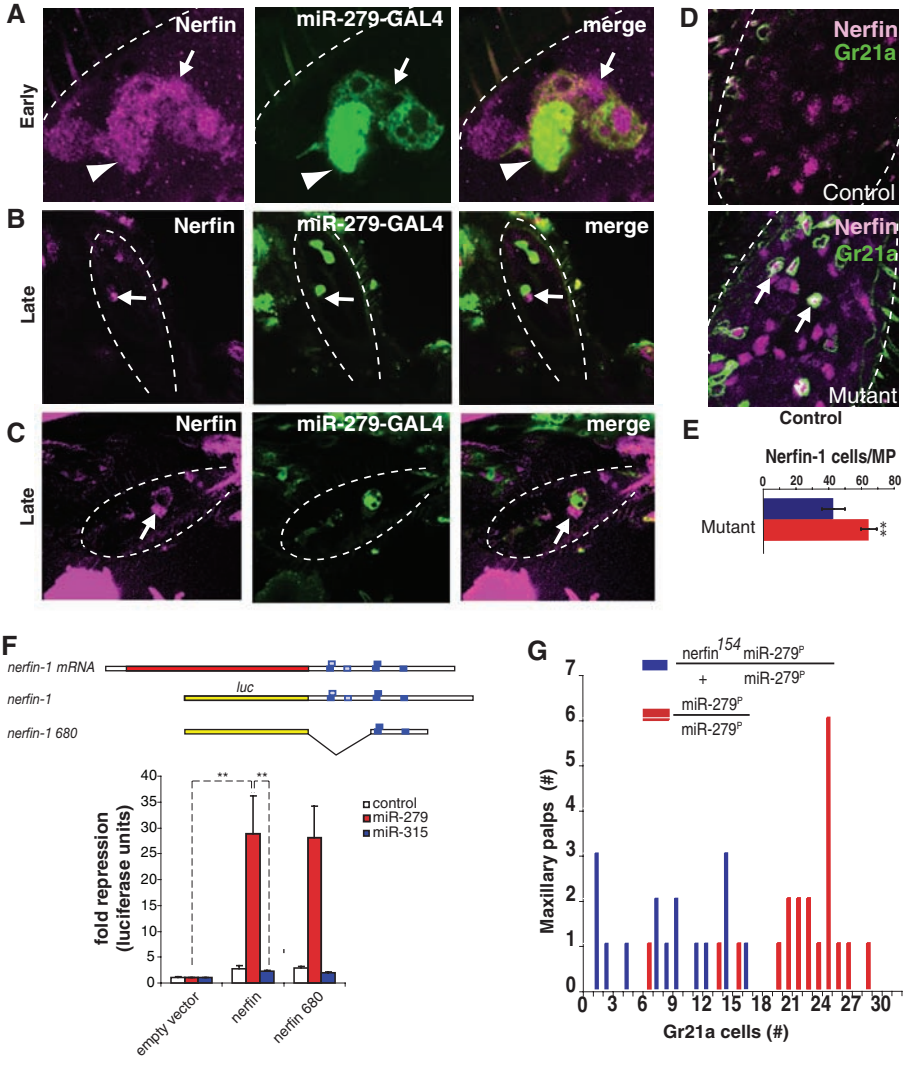

Fig. 3. Nerfin-1 is a target of *miR-279*. (**A** to **C**) Expression pattern of Nerfin-1 (magenta) and *miR-279* (green, see Fig. 2) in developing MPs at early (A) and later [(B) and (C)] stages. (**D**) Nerfin-1 (magenta) is expressed in ectopic CO_2 neurons (green) in the mutant MPs (arrows). (**E**) Quantification of Nerfin-1–positive nuclei in wild-type and mutant MPs at 60 to 80 hours APF. MPs scored: wild type, $n = 7$; mutant $n = 9$; $^{**}P < 0.001$. (**F**) *miR-279* inhibits *nerfin-1* expression in cultured *Drosophila* S2 cell lines ($^{**}P < 0.001$). (**G**) *nerfin-1* is a dominant suppressor of *miR-279* ($P < 0.001$).

flies carrying a transcriptional reporter construct (miR-279-GAL4). Expression was monitored in flies carrying this GAL4 construct and the reporter UAS-mCD8GFP (Fig. 2 and fig. S4). Around 40 to 50 hours after puparium formation (APF), large cells reminiscent of sensory organ precursors in other epithelia expressed *miR-279* (Fig. 2 and fig. S4). At later stages, miR-279–expressing cells were found in clusters with smaller cells, some of which expressed neuronal markers (fig. S4). As ORNs matured, *miR-279* expression was lost (fig. S4).

We next sought to identify the target gene(s) responsible for the *miR-279* mutant phenotype. About 205 potential target mRNAs of *miR-279* were previously predicted (*12*, *13*). One of the strongest candidates for *miR-279* regulation is Nerfin-1. The Nerfin-1 3′UTR contains multiple *miR-279* binding sites (Fig. 3F) and encodes a transcription factor expressed in neuronal precursors and transiently in nascent neurons in the embryonic central nervous system (*14*). Nerfin-1 protein appeared in *miR-279*–positive cells between 50 and 60 hours APF (Fig. 3A). Nerfin-1 and *miR-279* gradually redistributed, generating complementary expression patterns. Cells with high levels of Nerfin-1 expressed low levels of *miR-279* and vice versa (Fig. 3, B and C, and fig. S5).

To test whether Nerfin-1 is up-regulated in *miR-279* mutants, we stained mutant MPs with antibodies to Nerfin-1. We found 22 ± 4.8 additional Nerfin-1–expressing cells in *miR-279* mutant MPs relative to controls (Fig. 3E). This is similar to the number of ectopic CO_2 neurons in the MP (Fig. 1B). The vast majority of CO_2 ORNs in the MP expressed Nerfin-1 (Fig. 3D and fig. S5). Thus, the expression pattern of Nerfin-1 protein in the wild type and in mutant MPs is consistent with *nerfin-1* mRNA being a target for *miR-279* in vivo.

To determine whether *miR-279* directly binds to *nerfin-1* 3′UTR and inhibits its expression, we used a luciferase reporter assay in cultured cells. The luciferase-coding region was fused to the full-length *nerfin-1* 3′UTR, which contains four conserved 8-nucleotide oligomer target sites for *miR-279* (*15*), as well as to a subregion containing three of these sites (Fig. 3F). Luciferase activity of both *nerfin-1* sensor constructs was strongly repressed when cells were cotransfected with *miR-279* (Fig. 3F). By contrast, the activity of either *nerfin-1* sensor was unaffected by noncognate *miR-315*. Antisense oligomers directed against the *miR-279* core sequence specifically relieved *nerfin-1* reporter repression (fig. S6). Thus, we conclude that *nerfin-1* is a direct target of *miR-279*.

We next assessed whether Nerfin-1 down-regulation by *miR-279* inhibits the development of CO_2 neurons in the MPs. To do this, we reduced the level of *nerfin-1* by half genetically in a *miR-279* mutant background. This decreased the number of CO_2 neurons in the MP relative to *miR-279* mutants (Fig. 3G), providing strong in

Downloaded from http://science.sciencemag.org/ on October 17, 2017

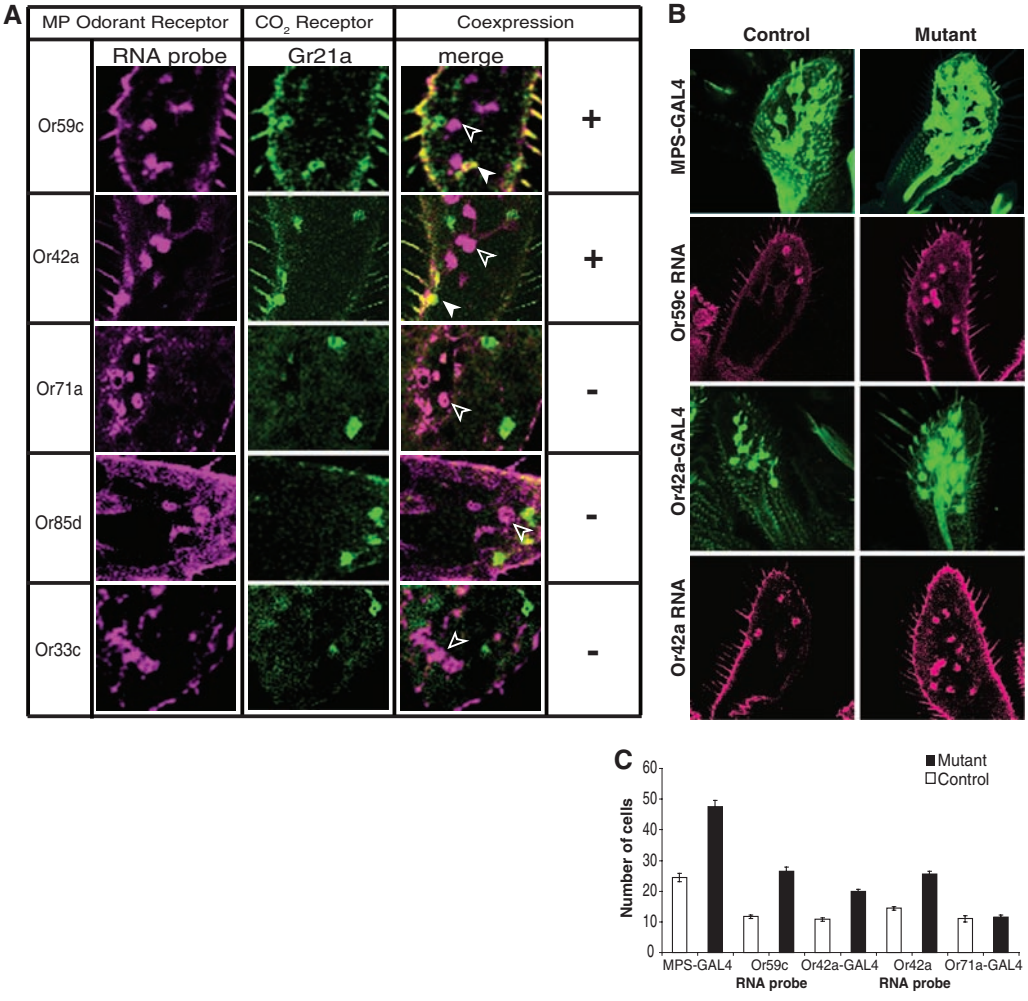

Fig. 4. Ectopic neurons exhibit mixed sensory identity. (**A**) MPs of mutant flies labeled with RNA antisense probes (magenta) and with Gr21a-GAL4 and UAS-mCD8GFP (green). Or59c and Or42a transcript (magenta) overlaps partly with Gr21a-expressing cells (green, solid arrowhead). Cells only positive for Or59c or Or42a are labeled only in magenta (open arrowhead). (**B** and **C**) MPs of mutant flies contain more Or42a- and Or59c-expressing cells. (B) Labeling of MP ORNs with GAL4 reporter constructs (Or42a-GAL4 and MPS-GAL4) or Or59c or Or42a RNA probe. (C) Quantification of the data from (B). Total increase in the number of cells in mutants using MPS-GAL4 driver corresponds to the number of ectopic CO_2 neurons (see Fig. 1B).

vivo evidence that *miR-279* is necessary to down-regulate Nerfin-1 in MPs during normal development. Nerfin-1 up-regulation alone was not sufficient to generate a miR-279–like phenotype (fig. S7). Taken together, these findings suggest that *miR-279* down-regulates Nerfin-1 and other targets to prevent CO_2 neuron development in the MPs.

When analyzing the axonal projections of the CO_2 neurons in the MPs, we observed that these neurons targeted one or more medial glomeruli in addition to the V-glomerulus, the target of antennal CO_2 neurons (Fig. 1F and fig. S2). These medial glomeruli are normally innervated by MP Or42a and Or59c ORNs. Double-labeling experiments revealed that mutant neurons also coexpressed Or42a and Or59c, but not other MP ORs (Fig. 4A). Analysis of subsets of MP ORNs also revealed that Or42a and Or59c classes each showed an approximate increase of 10 cells in the MPs, whereas others were unaffected (Fig. 4, B and C). These results indicate that the ectopic CO_2 neurons are formed as additional cells within Or42a and Or59c sensilla and are hybrid in identity. They express ORs and exhibit wiring characteristics of two classes of neurons.

It is interesting that the loss of *miR-279* generates a CO_2 neuron within a sensillum harboring four neurons in the MP (Fig. 1E and fig. S1), given that the antennal CO_2 sensilla in *Drosophila* are the only sensilla in the olfactory system to harbor four ORNs (*16*). Because *miR-279* acts within the precursor cells in the MP to prevent Nerfin-dependent formation of olfactory neurons, this observation raises the intriguing possibility that positioning of CO_2 neurons on different olfactory appendages might have evolved through changes at the level of precursor cell development. Thus, the evolutionary elimination of CO_2 neurons from MP sensilla might have required decreasing the number of cells with neuronal identities through down-regulation of Nerfin-1 by *miR-279*.

Although we hypothesize that relocation of CO_2 ORNs to different appendages was important in the evolution of differences in CO_2 sensing, additional mechanisms must have evolved to modify the neural circuitry to alter species-specific behaviors in response to CO_2. The ectopic CO_2 neurons are hybrid cells, which express additional receptors (Or59c or Or42a) and also target medial glomeruli, typically innervated by wild-type ORNs expressing these ORs. This is particularly interesting given that CO_2 neurons in mosquitoes connect to medial glomeruli, driving an attractive response (*17*–*19*). We speculate that this hybrid cell represents an evolutionary intermediate on a path leading to species-specific CO_2 behavior (*20*). Perhaps suppressing the expression of Or59c or Or42a ORs could convert this hybrid cell to one dedicated only to CO_2 reception. The nature of the behavioral output to CO_2 (i.e., attraction versus repulsion) by this cell, however, may be dictated by altering the wiring specificity to one site or the other (medial versus ventral, respectively). More generally, we propose that natural selection can work on such an evolutionary intermediate to generate different combinations of OR, wiring, and cellular positional specificities, depending on the insects' environmental needs. This may in turn lead to novel olfactory responses to different odorants, or to the same odorant in different species.

References and Notes

1. F. E. Kellogg, *J. Insect Physiol.* **16**, 99 (1970).
2. A. J. Grant, R. J. O'Connell, *Ciba Found. Symp.* **200**, 233 (1996).
3. F. Bogner, *Physiol. Entomol.* **17**, 1992 (1992).
4. C. Thom, P. G. Guerenstein, W. L. Mechaber, J. G. Hildebrand, *J. Chem. Ecol.* **30**, 1285 (2004).
5. F. Bogner, M. Boppre, K. D. Ernst, J. Boeckh, *J. Comp. Physiol. A* **158**, 741 (1986).
6. G. S. Suh *et al.*, *Nature* **431**, 854 (2004).
7. W. D. Jones, P. Cayirlioglu, I. G. Kadow, L. B. Vosshall, *Nature* **445**, 86 (2007).

Downloaded from http://science.sciencemag.org/ on October 17, 2017

8. J. Y. Kwon, A. Dahanukar, L. A. Weiss, J. R. Carlson, *Proc. Natl. Acad. Sci. U.S.A.* **104**, 3574 (2007).
9. See supporting material on *Science* Online.
10. L. B. Vosshall, *Curr. Opin. Neurobiol.* **10**, 498 (2000).
11. K. S. Kosik, A. M. Krichevsky, *Neuron* **47**, 779 (2005).
12. A. Stark, J. Brennecke, R. B. Russell, S. M. Cohen, *PLoS Biol.* **1**, e60 (2003).
13. D. Grun, Y. L. Wang, D. Langenberger, K. C. Gunsalus, N. Rajewsky, *PLoS Comput. Biol.* **1**, e13 (2005).
14. A. Kuzin, T. Brody, A. W. Moore, W. F. Odenwald, *Dev. Biol.* **277**, 347 (2005).
15. B. P. Lewis, C. B. Burge, D. P. Bartel, *Cell* **120**, 15 (2005).
16. A. Couto, M. Alenius, B. J. Dickson, *Curr. Biol.* **15**, 1535 (2005).
17. S. Anton *et al.*, *Arthropod Struct. Dev.* **32**, 319 (2003).
18. P. Distler, J. Boeckh, *J. Exp. Biol.* **200**, 1873 (1997).
19. R. Ignell, T. Dekker, M. Ghaninia, B. S. Hansson, *J. Comp. Neurol.* **493**, 207 (2005).
20. F. J. Poelwijk, D. J. Kiviet, D. M. Weinreich, S. J. Tans, *Nature* **445**, 383 (2007).
21. We thank L. Vosshall, B. Dickson, W. Odenwald, R. Klein, G. Tavosanis, J. Carlson, and D. Anderson for providing reagents and comments on experiments; W. Tom, A. Lorenze, and P. Alcala for technical assistance; A. Acker-Palmer, T. Suzuki, G. Tavosanis, R. Klein, and members of the laboratories for comments on the manuscript; A. Luke for helping with *miR-279* deletions; and Y.-T. Chou for cloning the luciferase sensors. Supported by the Jane Coffin Childs Memorial Fund and a National Research Service Award (P.C.); EMBO and the Human Frontiers Science Program (I.G.K.); the Leukemia and Lymphoma Foundation, the Burroughs Wellcome Foundation, and the V-Foundation for Cancer Research (E.C.L.); and NIH grant DC006485 (S.L.Z.). G.S.B.S. is an HHMI Associate; S.L.Z. is an HHMI Investigator.

Supporting Online Material
www.sciencemag.org/cgi/content/full/319/5867/1256/DC1
Materials and Methods
Figs. S1 to S7
References

20 August 2007; accepted 17 January 2008
10.1126/science.1149483

Transgenic Inhibition of Synaptic Transmission Reveals Role of CA3 Output in Hippocampal Learning

Toshiaki Nakashiba, Jennie Z. Young, Thomas J. McHugh, Derek L. Buhl, Susumu Tonegawa*

The hippocampus is an area of the brain involved in learning and memory. It contains parallel excitatory pathways referred to as the trisynaptic pathway (which carries information as follows: entorhinal cortex → dentate gyrus → CA3 → CA1 → entorhinal cortex) and the monosynaptic pathway (entorhinal cortex → CA1 → entorhinal cortex). We developed a generally applicable tetanus toxin–based method for transgenic mice that permits inducible and reversible inhibition of synaptic transmission and applied it to the trisynaptic pathway while preserving transmission in the monosynaptic pathway. We found that synaptic output from CA3 in the trisynaptic pathway is dispensable and the short monosynaptic pathway is sufficient for incremental spatial learning. In contrast, the full trisynaptic pathway containing CA3 is required for rapid one-trial contextual learning, for pattern completion–based memory recall, and for spatial tuning of CA1 cells.

The medial temporal lobes of the brain, including the hippocampus, are crucial for learning and memory of events and space across species (*1*–*3*). The hippocampus receives input from virtually all associative areas of the neocortex via the entorhinal cortex (EC). In the main excitatory hippocampal network (Fig. 1A), information flows from the superficial layer (layer II) of the EC to the dentate gyrus (DG) to CA3 to CA1 and finally to the deep layers of EC directly or indirectly through the subiculum. This loop is referred to as the trisynaptic pathway (TSP). The hippocampus also contains a parallel excitatory monosynaptic pathway (MSP) [EC (layer III) → CA1 → EC (layer V)] as well as other excitatory and inhibitory circuits.

The prevailing view of the contribution of these circuits to hippocampal function (*4*–*7*) is that synaptic transmission and plasticity in the feed-forward pathway from EC → DG → CA3, a part of the TSP, are primarily responsible for pattern separation, whereas those in a recurrent network within CA3 are crucial for the rapid association of diverse sets of information and pattern completion. Furthermore, CA1 may be instrumental in recognizing the novelty of an event or context (*8*, *9*).

Some of these ideas have been tested by lesioning (*10*) portions of the hippocampus or EC, although it is difficult to restrict damage to specific subregions and cell types in a quantitative and reproducible manner (*11*, *12*). These difficulties have in part been addressed by deleting the *N*-methyl-D-aspartate (NMDA) receptor gene *NR1* in specific hippocampal subregions with Cre-loxP recombination technology. These studies found that NMDA receptor–dependent synaptic plasticity in postnatal excitatory neurons of each of several hippocampal subregions is required for specific aspects of hippocampal learning and memory (*13*–*16*). In order to completely analyze hippocampal function, we developed a method to block neural transmission rather than synaptic plasticity and used it to assess the differential role of CA3 and EC outputs into area CA1 in hippocampus-dependent learning and memory.

We generated a triple transgenic mouse (Fig. 1B) by doxycycline (Dox)–inhibited circuit exocytosis knockdown (DICE-K), in which synaptic transmission is blocked by cell type–restricted and temporally controlled expression of the tetanus toxin (TeTX) light chain (*17*). TeTX is an endopeptidase specific for VAMP2 (*18*), which is essential for activity-dependent neurotransmitter release from presynaptic terminals (*19*). The rationale for this general method is described fully in the supporting online material (SOM).

We used the KA1 promoter (*14*) and α-CaMKII promoter (*20*) for the transgenic1 (Tg1) and transgenic2 (Tg2) mice, respectively, to block CA3 output in the TSP while keeping EC output in the MSP intact (Fig. 1B). Before generating the triple transgenic TeTX mouse line, we investigated several parameters of the DICE-K method by crossing the Tg1×Tg2 double transgenic mouse with a Tg3–green fluorescent protein (GFP) reporter line (CA3-GFP) (Fig. 1B). Immunohistology (Fig. 1, C to H) indicated that GFP expression was restricted to CA3 and DG in mice maintained on a Dox-free diet (Fig. 1, C to E). There was no expression of GFP in the CA1 pyramidal cell layer [stratum (s.) pyramidale] or temporoammonic (TA) pathway (s. lacunosum moleculare) but abundant expression in the Schaffer collateral (SC) pathway (s. radiatum and s. oriens) (Fig. 1E). In the Tg1×Tg2 mouse, the spatial restriction was much greater than in the Tg1 mouse (fig. S1). GFP expression was repressed in the Dox-on state (Fig. 1F), de-repressed in the Dox-on-off state (Fig. 1G), and re-repressed in the Dox-on-off-on state (Fig. 1H).

We crossed Tg1×Tg2 double transgenic mice with Tg3-TeTX mice to produce a triple transgenic mouse, CA3-TeTX. In hippocampal slices from control double transgenic mice (Tg1×Tg3-TeTX), VAMP2 immunoreactivity (IR) was observed where axonal terminals are known to exist (Fig. 1, I and M). Hippocampal VAMP2 IR patterns were indistinguishable between repressed CA3-TeTX and control mice (Fig. 1J). In hippocampal slices from CA3-TeTX mice that had been on Dox followed by 4 weeks of Dox withdrawal, there was a striking reduction of VAMP2 IR in the s. radiatum and s. oriens of CA1 and CA3 and in the inner one-third of the molecular layer (ML) of DG, but not in other strata (Fig. 1K). Similar patterns of VAMP2 IR were observed in hippocampal slices throughout the dorsoventral axis. The CA3-SC innervates CA1 in the s. radiatum and s. oriens, whereas CA3-recurrent collateral (RC) innervates CA3 in these

The Picower Institute for Learning and Memory, Howard Hughes Medical Institute, RIKEN-MIT Neuroscience Research Center, Department of Biology and Department of Brain and Cognitive Sciences, Massachusetts Institute of Technology, Cambridge, MA 02139, USA.

*To whom correspondence should be addressed. E-mail: tonegawa@mit.edu

Downloaded from http://science.sciencemag.org/ on October 17, 2017

ERRATUM

Post date 20 June 2008

Reports: "Hybrid neurons in a microRNA mutant are putative evolutionary intermediates in insect CO_2 sensory systems" by P. Cayirlioglu *et al*. (29 February, p. 1256). The introductory paragraph incorrectly stated that CO_2 neurons in the tsetse fly are located in the maxillary palps. They are found in the antennae.

Downloaded from http://science.sciencemag.org/ on October 17, 2017

Science

Hybrid Neurons in a MicroRNA Mutant Are Putative Evolutionary Intermediates in Insect CO_2 Sensory Systems

Pelin Cayirlioglu, Ilona Grunwald Kadow, Xiaoli Zhan, Katsutomo Okamura, Greg S. B. Suh, Dorian Gunning, Eric C. Lai and S. Lawrence Zipursky

Science **319** (5867), 1256-1260.
DOI: 10.1126/science.1149483

ARTICLE TOOLS http://science.sciencemag.org/content/319/5867/1256

SUPPLEMENTARY MATERIALS http://science.sciencemag.org/content/suppl/2008/02/28/319.5867.1256.DC1

RELATED CONTENT http://stke.sciencemag.org/content/sigtrans/1/9/ec85.abstract
http://science.sciencemag.org/content/sci/320/5883/1588.1.full
http://stke.sciencemag.org/contenthttp://stke.sciencemag.org/cgi/content/abstract/sigtrans;1/9/ec85

REFERENCES This article cites 19 articles, 2 of which you can access for free
http://science.sciencemag.org/content/319/5867/1256#BIBL

PERMISSIONS http://www.sciencemag.org/help/reprints-and-permissions

Use of this article is subject to the Terms of Service

Science (print ISSN 0036-8075; online ISSN 1095-9203) is published by the American Association for the Advancement of Science, 1200 New York Avenue NW, Washington, DC 20005. 2017 © The Authors, some rights reserved; exclusive licensee American Association for the Advancement of Science. No claim to original U.S. Government Works. The title *Science* is a registered trademark of AAAS.

Downloaded from http://science.sciencemag.org/ on October 17, 2017